

Modal Power Flow Analysis of a Damaged
Orthotropic Plate

by

Waion Wong, Yanlung Cheung and Li Cheng

Reprinted from

Advances in Structural Engineering

Volume 16 No. 1 2013

MULTI-SCIENCE PUBLISHING CO. LTD.
5 Wates Way, Brentwood, Essex CM15 9TB, United Kingdom

Modal Power Flow Analysis of a Damaged Orthotropic Plate

Waion Wong*, Yanlung Cheung and Li Cheng

Department of Mechanical Engineering, The Hong Kong Polytechnic University, Hong Kong, China

Abstract: The effect of the change of structural integrity to the change of the reactive power flow of a vibrating structure at resonance is explored both analytically and numerically. When an undamped structure undergoes free vibration at one of its natural frequencies, the reactive component is of modal pattern and it can be used as a new modal signature. The reactive power flow in this case can thus be termed as modal power flow. The instantaneous energy density associated with the vibration mode consists of a static component and a dynamic component, related to the mean total and Lagrangian energy densities, respectively. The modal power flow is relevant to the latter but independent of the former. The inverse problem of detecting structural damage due to the identification of variation of modal power flow pattern is investigated. Modal power flow of an orthotropic composite plate with a region of reduced stiffness in the plate is analyzed. Numerical tests show that the proposed method is effective for detection of the damage and the modal power flow is more sensitive to the change of plate stiffness than the strain mode shape in the test cases.

Key words: power flow, damage, composite.

1. INTRODUCTION

Composite panels are popularly used in transport systems like aircraft and trains because of their light-weight and high-rigidity. Delamination is a common type of damage in composite panels. Detection of damage occurring in composite panels is an important topic in mechanical and structural engineering applications (Alvandi and Cremona 2006; Zou *et al.* 2000). Identification of damage location is the basic step for damage repair and control and many techniques have been developed for that purpose in recent years (Chen and Bicanic 2000; Li *et al.* 2002; Shi *et al.* 1998; Cornwell *et al.* 1999). A relatively new technique is based on the study of power flow or structural intensity in a vibrating structure. There are in general active and reactive powers presented in a vibrating structure. Active power is defined as the product of a generalized force with the in-phase component of a generalized velocity, where the velocity is in the same direction as the force. Forces and velocities in a vibrating structure will be exactly 90 degrees out of phase if no damping and no

energy dissipation such as sound radiation in the system is assumed. The product of the corresponding force and velocity terms is called the reactive power which represents the amount of energy stored in the structure (Mandal and Biswas 2005).

Li *et al.* (2001) proposed the diagnosis of flaws in damaged beam structures using vibrational power flow. Khun *et al.* (2004) showed that loosened bolt joints in plate assembly could be identified from the power flow pattern in the plates. Lee *et al.* (2006) calculated the diversion of energy flow near crack tips of a vibrating plate using structural intensity technique. They showed that the presence of a crack can be identified by the changes of the directions of SI vectors near the crack. In all these reported methods, however, the forced vibration data of an excited structure were required. Accordingly, it was the active power flow which was used for damage identification. There is no report found in the literature about the use of reactive power flow in a plate for damage identification.

*Corresponding author. Email address: mmwong@polyu.edu.hk; Fax: +852 2365 4703; Tel: +852 2766 6667.

The aim of this paper is to study the power flow and energy distribution of a vibration mode of a damaged composite plate. The power flow is shown to be of reactive nature in this case, and referred to as the modal power flow in the following. The outline of this paper is as follows. In section 2, the modal power flow analysis of the damaged plate is performed, and the relation between the modal power flow and the modal energy distribution in the plate is derived. The modal power flow is proposed to locate damage sites in plate-like structures. In section 3, some numerical simulations are demonstrated to analyze the identification capability of the proposed damage indicator. Finally, conclusions are drawn.

2. MODAL POWER FLOW ANALYSIS OF A DAMAGED PLATE

From plate theory, the equation of motion of a thin vibrating orthotropic plate may be written as

$$\left(D_x \frac{\partial^4 w}{\partial x^4} + 2H \frac{\partial^4 w}{\partial x^2 \partial y^2} + D_y \frac{\partial^4 w}{\partial y^4} \right) + \rho h \frac{\partial^2 w}{\partial t^2} = 0 \quad (1)$$

where $D_x = \frac{E_x h^3}{12(1-\nu_x \nu_y)}$, $D_y = \frac{E_y h^3}{12(1-\nu_y \nu_x)}$, $H = \nu_x D_y + 2D_{xy}$ and $D_{xy} = G_{xy} h^3 / 12$, in which E_x and E_y are the moduli of elasticity in the x and y directions respectively, G_{xy} is the shear modulus, ν_x and ν_y are Poisson ratios, h is the thickness of the plate, and ρ is the material density. D_x and D_y are called the flexural rigidities and D_{xy} is the torsional rigidity of the plate, $2H$ is called the effective torsional rigidity of the orthotropic plate, and w is the transverse deflection in the z -direction.

Assuming the plate has a harmonic motion of frequency ω , its displacement may be written as

$$w(x, y; t) = W(x, y) \sin \omega t \quad (2)$$

where $W(x, y)$ is the vibration amplitude of the plate.

The strain distributions of the plate may be written as

$$\begin{aligned} \Psi_x(x, y) &= \frac{\partial^2 W(x, y)}{\partial x^2}, \quad \Psi_y(x, y) = \frac{\partial^2 W(x, y)}{\partial y^2}, \\ \Psi_{xy}(x, y) &= \frac{\partial^2 W(x, y)}{\partial x \partial y}. \end{aligned} \quad (3)$$

The instantaneous power flow at point (x, y) may be written as [11]

$$\vec{P}(x, y; t) = P_x(x, y; t) \vec{i} + P_y(x, y; t) \vec{j} \quad (4)$$

where

$$\begin{aligned} P_x(x, y; t) &= \frac{\partial}{\partial x} \left(D_x \frac{\partial^2 w}{\partial x^2} + H \frac{\partial^2 w}{\partial y^2} \right) \dot{w} \\ &\quad - D_x \left(\frac{\partial^2 w}{\partial x^2} + \nu_y \frac{\partial^2 w}{\partial y^2} \right) \frac{\partial \dot{w}}{\partial x} \\ &\quad - 2D_{xy} \frac{\partial^2 w}{\partial x \partial y} \frac{\partial \dot{w}}{\partial y}, \text{ and} \end{aligned} \quad (5)$$

$$\begin{aligned} P_y(x, y; t) &= \frac{\partial}{\partial y} \left(D_y \frac{\partial^2 w}{\partial y^2} + H \frac{\partial^2 w}{\partial x^2} \right) \dot{w} \\ &\quad - D_y \left(\frac{\partial^2 w}{\partial y^2} + \nu_x \frac{\partial^2 w}{\partial x^2} \right) \frac{\partial \dot{w}}{\partial y} \\ &\quad - 2D_{xy} \frac{\partial^2 w}{\partial y \partial x} \frac{\partial \dot{w}}{\partial x}. \end{aligned} \quad (6)$$

2.1. Relationship between Power Flow and Energy Distributions of a Vibrating Plate

Eqn 5 may be rewritten using Eqns 2 and 3 as

$$\begin{aligned} P_x(x, y; t) &= \frac{\partial}{\partial x} \left(D_x \frac{\partial^2 w}{\partial x^2} + H \frac{\partial^2 w}{\partial y^2} \right) \dot{w} \\ &\quad - D_x \left(\frac{\partial^2 w}{\partial x^2} + \nu_y \frac{\partial^2 w}{\partial y^2} \right) \frac{\partial \dot{w}}{\partial x} - 2D_{xy} \frac{\partial^2 w}{\partial x \partial y} \frac{\partial \dot{w}}{\partial y} \\ &= \frac{1}{2} \omega \left[\frac{\partial(D_x \Psi_x + H \Psi_y)}{\partial x} W \right. \\ &\quad \left. - D_x (\Psi_x + \nu_y \Psi_y) \frac{\partial W}{\partial x} - 2D_{xy} \Psi_{xy} \frac{\partial W}{\partial y} \right] \\ &\quad \times \sin 2\omega t = P_{x_max} \sin 2\omega t \end{aligned} \quad (7a)$$

where

$$\begin{aligned} P_{x_max} &= \frac{1}{2} \omega \left[\frac{\partial(D_x \Psi_x + H \Psi_y)}{\partial x} W \right. \\ &\quad \left. - D_x (\Psi_x + \nu_y \Psi_y) \frac{\partial W}{\partial x} \right. \\ &\quad \left. - 2D_{xy} \Psi_{xy} \frac{\partial W}{\partial y} \right] \end{aligned} \quad (7b)$$

Eqn 6 may be rewritten using Eqns 2 and 3 as

$$\begin{aligned}
 P_y(x,y;t) &= \frac{\partial}{\partial y} \left(D_y \frac{\partial^2 w}{\partial y^2} + H \frac{\partial^2 w}{\partial x^2} \right) \dot{w} \\
 &\quad - D_y \left(\frac{\partial^2 w}{\partial y^2} + \nu_x \frac{\partial^2 w}{\partial x^2} \right) \frac{\partial \dot{w}}{\partial y} - 2D_{xy} \frac{\partial^2 w}{\partial y \partial x} \frac{\partial \dot{w}}{\partial x} \\
 &= \frac{1}{2} \omega \left[\frac{\partial(D_y \Psi_y + H \Psi_x)}{\partial y} W \right. \\
 &\quad \left. - D_y (\Psi_y + \nu_x \Psi_x) \frac{\partial W}{\partial y} - 2D_{xy} \Psi_{xy} \frac{\partial W}{\partial x} \right] \\
 &\quad \times \sin 2\omega t \\
 &= P_{y_max} \sin 2\omega t
 \end{aligned} \tag{8a}$$

$$\begin{aligned}
 \text{where } P_{y_max} &= \frac{1}{2} \omega \left[\frac{\partial(D_y \Psi_y + H \Psi_x)}{\partial y} W \right. \\
 &\quad \left. - D_y (\Psi_y + \nu_x \Psi_x) \frac{\partial W}{\partial y} - 2D_{xy} \Psi_{xy} \frac{\partial W}{\partial x} \right] \tag{8b}
 \end{aligned}$$

The power gradients may be written as

$$\begin{aligned}
 \frac{\partial P_x}{\partial x} &= \frac{1}{2} \omega \left[\frac{\partial^2 (D_x \Psi_x + H \Psi_y)}{\partial x^2} W \right. \\
 &\quad + \frac{\partial(D_x \Psi_x + H \Psi_y)}{\partial x} \frac{\partial W}{\partial x} \\
 &\quad - D_x \left(\frac{\partial \Psi_x}{\partial x} + \nu_y \frac{\partial \Psi_y}{\partial x} \right) \frac{\partial W}{\partial x} \\
 &\quad - D_x (\Psi_x + \nu_y \Psi_y) \Psi_x - 2D_{xy} \Psi_{xy} \Psi_{xy} \\
 &\quad \left. - 2D_{xy} \frac{\partial \Psi_{xy}}{\partial x} \frac{\partial W}{\partial y} \right] \sin 2\omega t
 \end{aligned} \tag{9}$$

and

$$\begin{aligned}
 \frac{\partial P_y}{\partial y} &= \frac{1}{2} \omega \left[\frac{\partial^2 (D_y \Psi_y + H \Psi_x)}{\partial y^2} W \right. \\
 &\quad + \frac{\partial(D_y \Psi_y + H \Psi_x)}{\partial y} \frac{\partial W}{\partial y} \\
 &\quad - D_y \left(\frac{\partial \Psi_y}{\partial y} + \nu_x \frac{\partial \Psi_x}{\partial y} \right) \frac{\partial W}{\partial y} \\
 &\quad - D_y (\Psi_y + \nu_x \Psi_x) \Psi_y - 2D_{xy} \Psi_{xy} \Psi_{xy} \\
 &\quad \left. - 2D_{xy} \frac{\partial \Psi_{xy}}{\partial y} \frac{\partial W}{\partial x} \right] \sin 2\omega t
 \end{aligned} \tag{10}$$

The power flow $\vec{P}(x,y;t)$ can be related to the instantaneous energy stored in the plate in the following. The distribution of the instantaneous kinetic energy of the plate may be written as

$$\begin{aligned}
 T &= \frac{1}{2} \rho h \omega^2 W^2 \cos^2 \omega t \\
 &= T_{max} \cos^2 \omega t
 \end{aligned} \tag{11}$$

$$\text{where } T_{max} = \frac{1}{2} \rho h \omega^2 W^2. \tag{12}$$

The distribution of the instantaneous strain energy of the plate may be written as

$$\begin{aligned}
 U &= \frac{1}{2} \omega \left[D_x \Psi_x^2 + D_y \Psi_y^2 + 2\nu_x D_y \Psi_x \Psi_y \right. \\
 &\quad \left. + 4D_{xy} (\Psi_{xy})^2 \right] \sin^2 \omega t \\
 &= U_{max} \sin^2 \omega t
 \end{aligned} \tag{13}$$

$$\begin{aligned}
 \text{where } U_{max} &= \\
 &= \frac{1}{2} \omega \left[D_x \Psi_x^2 + D_y \Psi_y^2 + 2\nu_x D_y \Psi_x \Psi_y + 4D_{xy} (\Psi_{xy})^2 \right].
 \end{aligned} \tag{14}$$

The instantaneous energy and distributions in the plate are written respectively as

$$\begin{aligned}
 E &= T_{max} \cos^2 \omega t + U_{max} \sin^2 \omega t \\
 &= \frac{1}{2} (T_{max} + U_{max}) + \frac{1}{2} (T_{max} - U_{max}) \cos 2\omega t, \text{ and} \\
 \frac{\partial E}{\partial t} &= \omega (T_{max} - U_{max}) \sin 2\omega t.
 \end{aligned} \tag{15}$$

Using Eqns 9 and 10, the sum of the power flow gradients can be written as

$$\begin{aligned}
 \frac{\partial P_x}{\partial x} + \frac{\partial P_y}{\partial y} &= \frac{1}{2} \omega \left[\frac{\partial^2 (D_x \Psi_x + H \Psi_y)}{\partial x^2} W \right. \\
 &\quad + \frac{\partial^2 (D_y \Psi_y + H \Psi_x)}{\partial y^2} W \\
 &\quad - D_x \Psi_x^2 - D_y \Psi_y^2 - 2\nu_x D_y \Psi_x \Psi_y \\
 &\quad \left. - 4D_{xy} (\Psi_{xy})^2 \right] \sin 2\omega t
 \end{aligned} \tag{17}$$

Eqn 1 may be rewritten using Eqn 2 as

$$D_x \frac{\partial^4 W}{\partial x^4} + 2H \left(\frac{\partial^2 W}{\partial x^2} \frac{\partial^2 W}{\partial y^2} \right) + D_y \frac{\partial^4 W}{\partial y^4} = \rho h \omega^2 W \quad (18)$$

Eqn 17 can be rewritten using Eqn 18 as

$$\begin{aligned} & \frac{\partial P_x}{\partial x} + \frac{\partial P_y}{\partial y} \\ &= \frac{1}{2} \omega \left\{ \rho h \omega^2 W^2 - \left[D_x \Psi_x^2 + D_y \Psi_y^2 \right. \right. \\ & \quad \left. \left. + 2\nu_x D_y \Psi_x \Psi_y + 4D_{xy} \left(\Psi_{xy} \right)^2 \right] \right\} \sin 2\omega t \end{aligned} \quad (19)$$

Using Eqns 12, 14 and 16, the instantaneous energy balance at a point (x, y) of the plate may be written as

$$\frac{\partial P_x}{\partial x} + \frac{\partial P_y}{\partial y} = \frac{\partial E}{\partial t} \quad (20)$$

The net power flow out of a region $x_1 \leq x \leq x_2$ and $y_1 \leq y \leq y_2$ can be obtained by integrating the above equation along x direction from x_1 to x_2 and along y direction from y_1 to y_2 and the result may be written as

$$\begin{aligned} & \int_{y_1}^{y_2} [P_x(x_2) - P_x(x_1)] dy + \int_{x_1}^{x_2} [P_y(y_2) - P_y(y_1)] dx \\ &= \omega \int_{y_1}^{y_2} \int_{x_1}^{x_2} (T_{\max} - U_{\max}) dx dy \sin 2\omega t \end{aligned} \quad (21)$$

This energy flow and balance in a region of the plate is illustrated in Figure 1.

Using Eqns 7, 8, 16 and 20, we may write

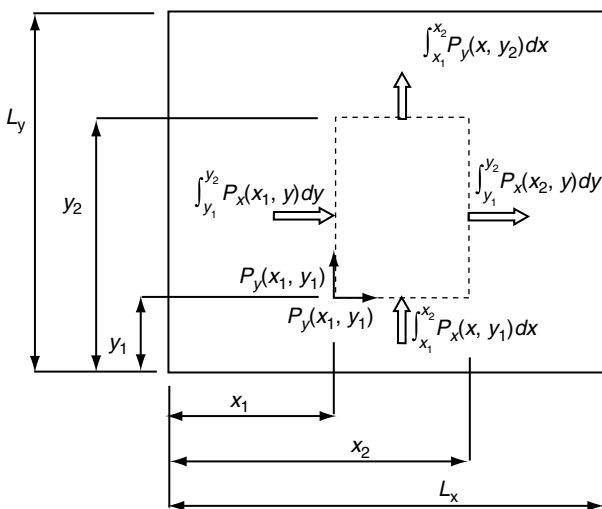


Figure 1. Illustration of the power flow in and out of a region (as shown by the hollow arrows) in a vibrating plate

$$\frac{\partial P_{x_{\max}}}{\partial x} + \frac{\partial P_{y_{\max}}}{\partial y} = \omega (T_{\max} - U_{\max}) \quad (22)$$

Eqn 22 shows that the sum of power flow gradients is proportional to the Lagrangian density $(T_{\max} - U_{\max})$ of the plate.

2.2. Modal Power Flow of a Plate

Since damping is neglected in the present analysis, the force and moment terms has no in-phase component of the corresponding velocity terms in the calculation of the power flow of a vibration mode of the plate. Therefore, the power flow of a vibration mode of the plate is the reactive power associated with that particular mode and it is termed as the modal power flow in the following analysis.

Using Eqns 4–6, the reactive power flow at the mn^{th} mode where $m, n = 1, 2, 3, \dots$, may be defined as

$$\begin{aligned} \vec{P}_{mn}(x, y; t) &= P_{mn_x}(x, y) \sin 2\omega_{mn} t \vec{i} \\ & \quad + P_{mn_y}(x, y) \sin 2\omega_{mn} t \vec{j} \end{aligned} \quad (23)$$

where

$$\begin{aligned} P_{mn_x}(x, y) &= \frac{\omega_{mn}}{2} \left[\left(D_x \frac{\partial^3 W_{mn}}{\partial x^3} + H \frac{\partial^3 W_{mn}}{\partial y^3} \right) W_{mn} \right. \\ & \quad - D_x \left(\frac{\partial^2 W_{mn}}{\partial x^2} + \nu \frac{\partial^2 W_{mn}}{\partial y^2} \right) \frac{\partial W_{mn}}{\partial x} \\ & \quad \left. - 2D_{xy} \frac{\partial^2 W_{mn}}{\partial x \partial y} \frac{\partial W_{mn}}{\partial y} \right] \end{aligned} \quad (24)$$

and

$$\begin{aligned} P_{mn_y}(x, y) &= \frac{\omega_{mn}}{2} \left[\left(D_y \frac{\partial^3 W_{mn}}{\partial y^3} + H \frac{\partial^3 W_{mn}}{\partial x^3} \right) W_{mn} \right. \\ & \quad - D_y \left(\frac{\partial^2 W_{mn}}{\partial y^2} + \nu \frac{\partial^2 W_{mn}}{\partial x^2} \right) \frac{\partial W_{mn}}{\partial y} \\ & \quad \left. - 2D_{xy} \frac{\partial^2 W_{mn}}{\partial y \partial x} \frac{\partial W_{mn}}{\partial x} \right] \end{aligned} \quad (25)$$

where ω_{mn} and W_{mn} are the natural frequency and mode shape of the mn^{th} vibration mode of the plate, respectively. From Eqn 20, the modal power flow can be related to the modal energy distribution of the plate as

$$\frac{\partial P_{mn-x}}{\partial x} + \frac{\partial P_{mn-y}}{\partial y} = \omega_{mn} (T_{mn-max} - U_{mn-max}) \quad (26)$$

where $T_{mn-max} = \frac{1}{2} \rho h \omega_{mn}^2 W_{mn}^2$ and (27)

$$U_{mn-max} = \frac{\omega_{mn}}{2} \left[D_x \left(\frac{\partial^2 W_{mn}}{\partial x^2} \right)^2 + D_y \left(\frac{\partial^2 W_{mn}}{\partial y^2} \right)^2 + 2\nu_x D_y \frac{\partial^2 W_{mn}}{\partial x^2} \frac{\partial^2 W_{mn}}{\partial y^2} + 4D_{xy} \left(\frac{\partial^2 W_{mn}}{\partial x \partial y} \right)^2 \right] \quad (28)$$

2.3. Damage Identification from the Modal Power Flow of a Plate

This part deals with the damage identification in a plate using the information about modal power flow. The basic concept is that a localized loss of stiffness will produce a curvature increase at the same location (Zou *et al.* 2000). If no change of mass in the damage region is assumed, this local change of curvature would induce a local change of bending strains (Li *et al.* 2002) and strain energy distribution (Shi *et al.* 1998) around the damage region resulting in the change of the gradients of power flow around the region as depicted by Eqn 26. This change of modal power flow may be more sensitive to the damage as it is a higher order derivative of the mode shape than the strain distribution of the plate (Whalen 2008).

The modal power flow vector field may be rewritten as

$$\frac{\vec{P}_{mn}(x, y; t)}{\omega_{mn}} = \left[\vec{P}_{mn-x}(x, y) \vec{i} + \vec{P}_{mn-y}(x, y) \vec{j} \right] \sin 2\omega_{mn} t \quad (29)$$

The vector field $\vec{P}_{mn}(x, y) / \omega_{mn} = \vec{P}_{mn-x} \vec{i} + \vec{P}_{mn-y} \vec{j}$ is proposed to be used for damage identification and location in plate-like structures. The advantage of using this term is that both the modal power flow components \vec{P}_{mn-x} and \vec{P}_{mn-y} can be derived by the mode shape data which can be obtained with a standard modal testing procedure (Ewins 2000).

3. SIMULATION ANALYSES

Modal power flow an orthotropic plate with a region of reduced stiffness in the plate is calculated according to the theory in Section 2. The vibration modes and hence

the modal power flow of a simply-supported rectangular plate with the damage are calculated with a self-developed *Matlab* program based on the Rayleigh-Ritz method (Li *et al.* 2002; Wong 2002). Changes of modal energy distributions and power flow due to the damage in a plate are compared and discussed in the following sections. Modal power flow and modal energy distributions are calculated according to Eqns 24, 25, 27 and 28.

3.1. Simulation of the Modal Power Flow in a Composite Plate

A simply-supported orthotropic square plate of size $1 \times 1 \times 0.01 \text{ m}^3$ is used in the simulation as illustrated in Figure 2(a). Figure 2(b) illustrates the presence of a region, $0.4 > x > 0.6$ and $0.4 > y > 0.6$, with stiffness reduction of 20% in the plate. It is assumed that $E_x/E_y = 10$ and $\nu_x = 0.25$. In applying the Rayleigh-Ritz method, the r^{th} mode shape function of the plate is expressed in a series written as (Li *et al.* 2002; Wong 2002)

$$W_r(x, y) = \sum_{i=1}^p \sum_{j=1}^q c_{r,ij} \cdot \varphi_i(x) \cdot \eta_j(y) \quad (30)$$

where $\varphi_i(x)$ and $\eta_j(y)$ are appropriate admissible functions, $c_{r,ij}$ the unknown coefficients. According to the Nyquist-Shannon sampling theorem (Marks 1991), $p = q = 20$ is applied in the calculation of the mode shape functions such that the highest spatial frequency of the admissible functions are twice of that used in the damaged region.

Contour plots of the calculated mode shape functions and modal energy distributions are generated and displayed by using the CONTOUR function in Matlab. Figures 2(c) and 2(d) show the contours of the vibration mode W_{11} of the intact and damaged plates respectively. No observable difference can be seen between Figures 2(c) and 2(d). Figures 2(e) and 2(f) show the contours of the strain modeshape ϵ_{11-x} of the intact and damaged plates respectively. Similar to the vibration modeshapes, there is no observable difference can be seen between the two strain modeshapes in Figures 2(e) and 2(f). Modal energy distributions of the plate are calculated according to Eqns 12 and 14. Figures 3(a) and 3(b) show the contours of the stationary modal energy distribution $T_{11-max} + V_{11-max}$ of the intact and damaged plates respectively. Some changes of the stationary energy can be observed in Figure 3(b) around the edges and the damaged region of the plate. Figures 3(c) and 3(d) show the contours of the Lagrangian density distribution $T_{11-max} - V_{11-max}$ of the intact and damaged plates respectively. Some changes of the stationary energy can

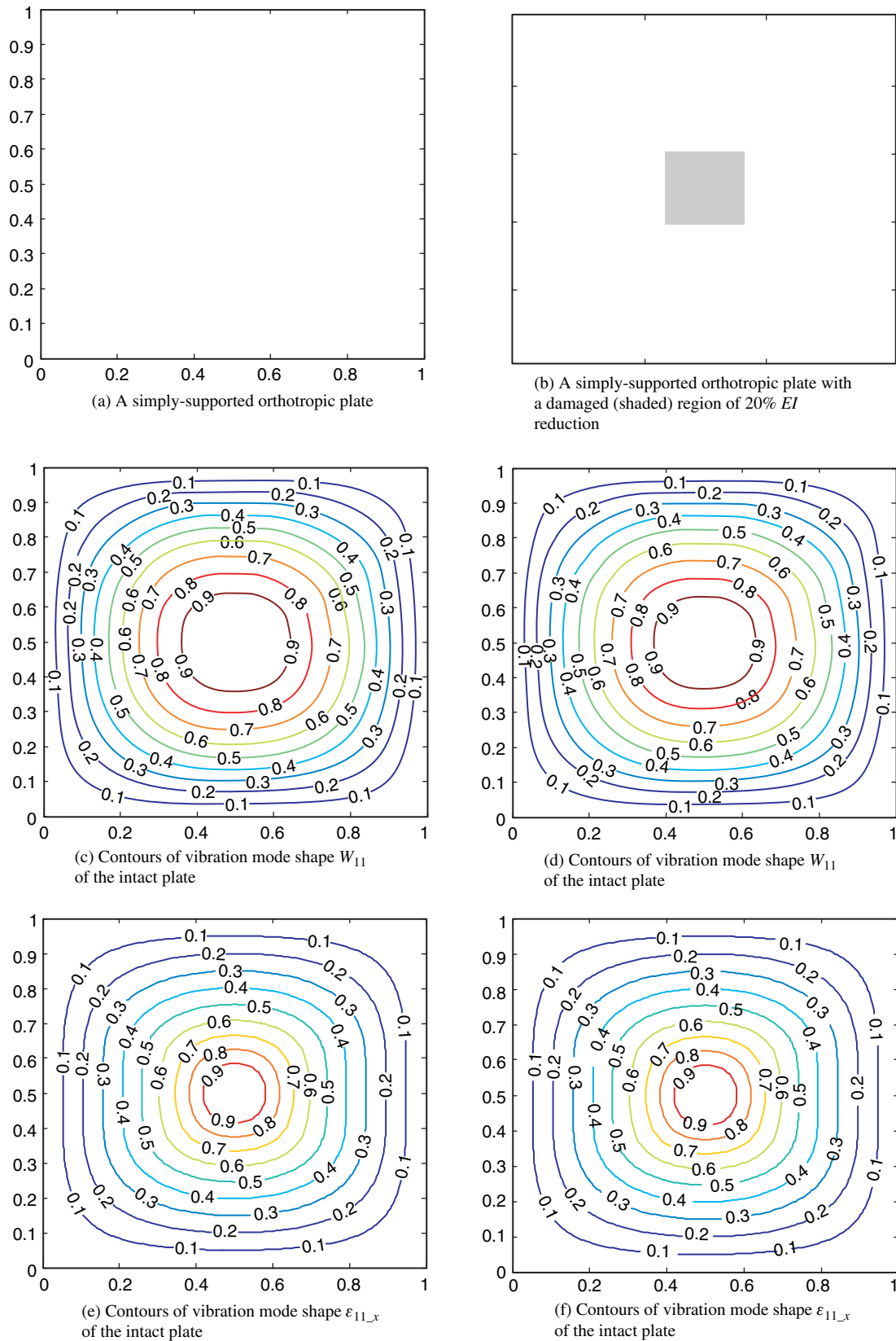


Figure 2. Comparison of the vibration mode shapes and strain mode shapes of a simply supported orthotropic composite plate with and without a damaged region

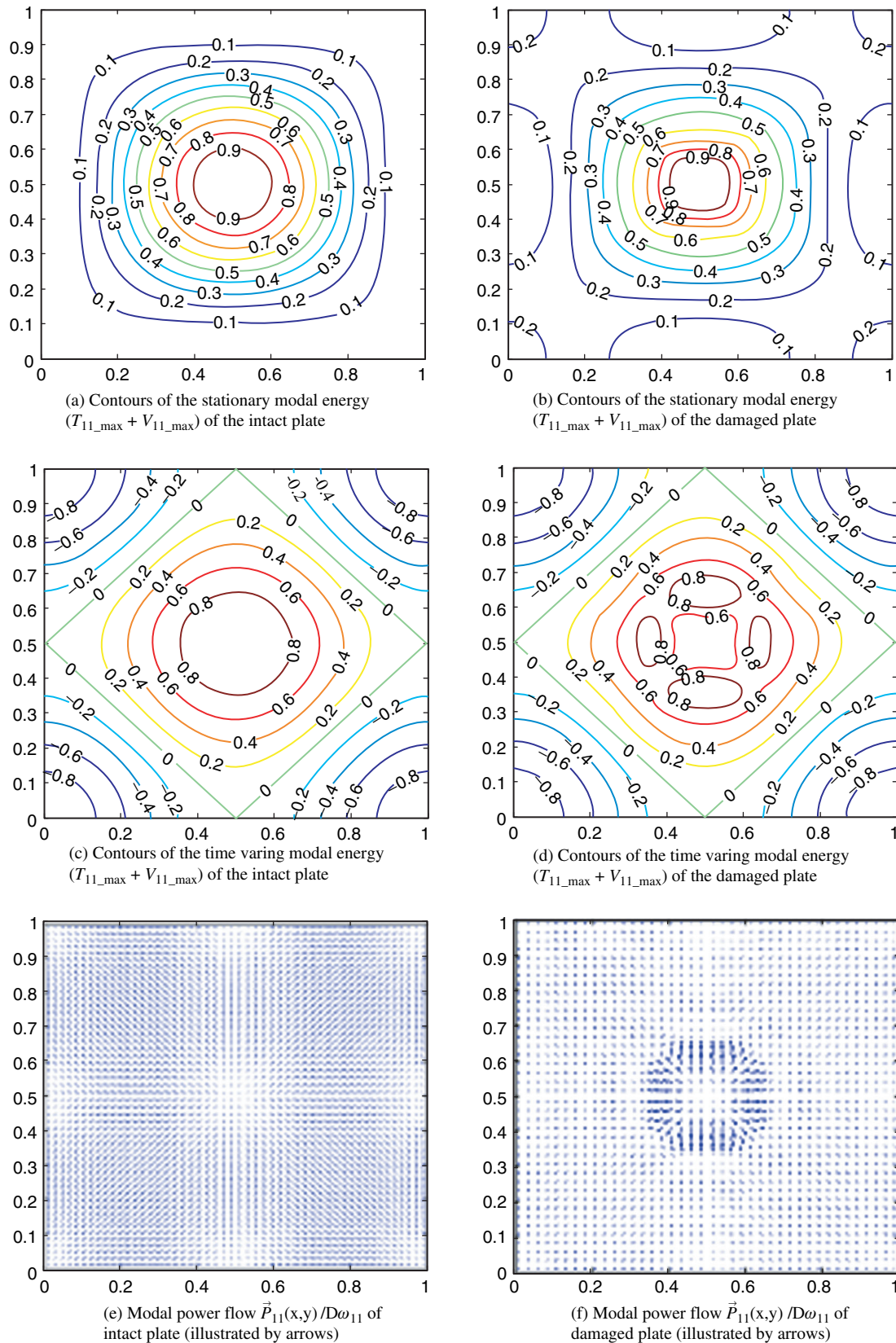


Figure 3. Comparison of the stationary modal energies, time varying modal energies and modal power flows of the simply supported orthotropic composite plate with [Figure 2(b)] and without [Figure 2(a)] a damaged region

be observed in Figure 3(d) around the damaged region of the plate. It should be noted that the modal power flow is proportional to the gradient of the Lagrangian density distribution; hence, the modal power flow would be more sensitive to a disturbance to the plate than the modal energy distribution. Figures 3(e) and 3(f) show the vector fields of the modal power flow $\vec{P}_{11}/D\omega_{11}$ of the intact and damaged plates respectively. It is observed in Figure 3(e) that power flow is smallest at the anti-nodes and the corners and power radiates in and out from the anti-nodes to the edges and the nodal line. Large vectors around the damaged region are observed in Figure 3(f) showing relatively large amount of energy flowing into and out of the damaged region.

3.2. Effect of Location and Size of the Damaged Region to the Change of Modal Power Flow in a Damaged Orthotropic Plate

Figure 4(a) illustrates the presence of a smaller damaged region, $0.175 > x > 0.325$ and $0.425 > y > 0.575$, with stiffness reduction of 20% in the plate. $p = q = 30$ is applied in the calculation of the mode shape functions such that the highest spatial frequency of the admissible functions are higher than twice of that used in the damaged region. Figure 4(b) plots the contours of the first vibration mode shape of the damaged plate. Figures 4(c) and 4(d) show the time-stationary modal energy distribution $T_{11_max} + V_{11_max}$ and the Lagrangian density distribution $T_{11_max} - V_{11_max}$, respectively. It is observed that the modal energy distribution $T_{11_max} + V_{11_max}$ increases whilst the Lagrangian density distribution decreases in the damage region. These effects would be a result of the increase of strain energy in the damage region as pointed out in Section 2.3. Figure 4(e) plots the contours of the first strain mode shape ε_{11_x} of the damaged plate. The damaged region cannot be identified based on the strain mode shape of the damaged plate. Figure 4(f) is a vector plot of the modal power flow in the damaged plate. Significant changes in amplitude and direction of the modal power flow can be observed in and around the damage region. These changes are consistent with the prediction as depicted by Eqn 26. Obviously, the modal power flow distribution is a local parameter sensitive to damage.

Figure 5(a) illustrates the presence of a region, $0.2 > x > 0.4$ and $0.2 > y > 0.4$, with stiffness reduction of 20% in the plate. Figure 5(b) plots the contours of the strain modeshape of the first vibration mode ε_{11_x} of the damaged composite plate. No indication of the damaged region can be observed from the strain modeshape. Figures 4(c) and 4(d) plots the contours of the modal

power flow flows P_{11_x} and P_{11_y} respectively of the damaged composite plate. Both P_{11_x} and P_{11_y} have local variations around the damaged region with the variations of P_{11_x} being more localized at the damaged region than that of P_{11_y} . It may due to the fact that the modulus along x – direction E_x is much higher than that along the y – direction and therefore the local variation of P_{11_y} extends further along the stiffer direction.

The two test cases as illustrated in Figures 4 and 5 have been studied again with less reduction of stiffness reduction at the damaged region (10% instead of 20%). Similar but lesser changes of the modal energies and power flow in comparison to those as shown in Figures 4 and 5 were observed. Contours plots of the modal energies and power flow looks similar to those in Figures 4 and 5 and therefore they are not plotted again.

4. CONCLUSIONS

Modal energy distributions and modal power flow in a damaged plate are studied, with the objective to demonstrate the capacity of modal power flow as a damage indicator. It is shown that the local time-averaged energy ($T_{max} + U_{max}$) increases at the damage region, hence the damage region behaves as an energy trap. Energy flowing in and out of the damage region to the surrounding regions may be increased or decreased depending on the location of the damage.

The capability for damage location identification for plate-like structures using modal reactive power flow is then demonstrated. Compared with the conventional damage indicators such as the change of strain mode shape of the plate, the proposed one is new and found to be more sensitive to the reduction of plate stiffness than the strain mode shape.

Moreover, compared with the damage identification techniques based on the determination of the active power flow in a damaged plate, the proposed method only requires information of a vibration mode shape of the structure and it is easier to apply in practice. Modal power flow of an orthotropic plate with a damaged region of reduced stiffness was analyzed. Numerical tests show that the modal power flow distribution is a local parameter sensitive to damage. The local variation of power flow is found to be relatively higher in the direction of smaller modulus in the damaged region of the orthotropic material and the local variation of modal power flow is found to extend further along the stiffer direction. The proposed power flow method may help to locate a damaged region in an orthotropic plate. Future research works would be experimental verification of the proposed theory and the possibility of quantification of the damage region.

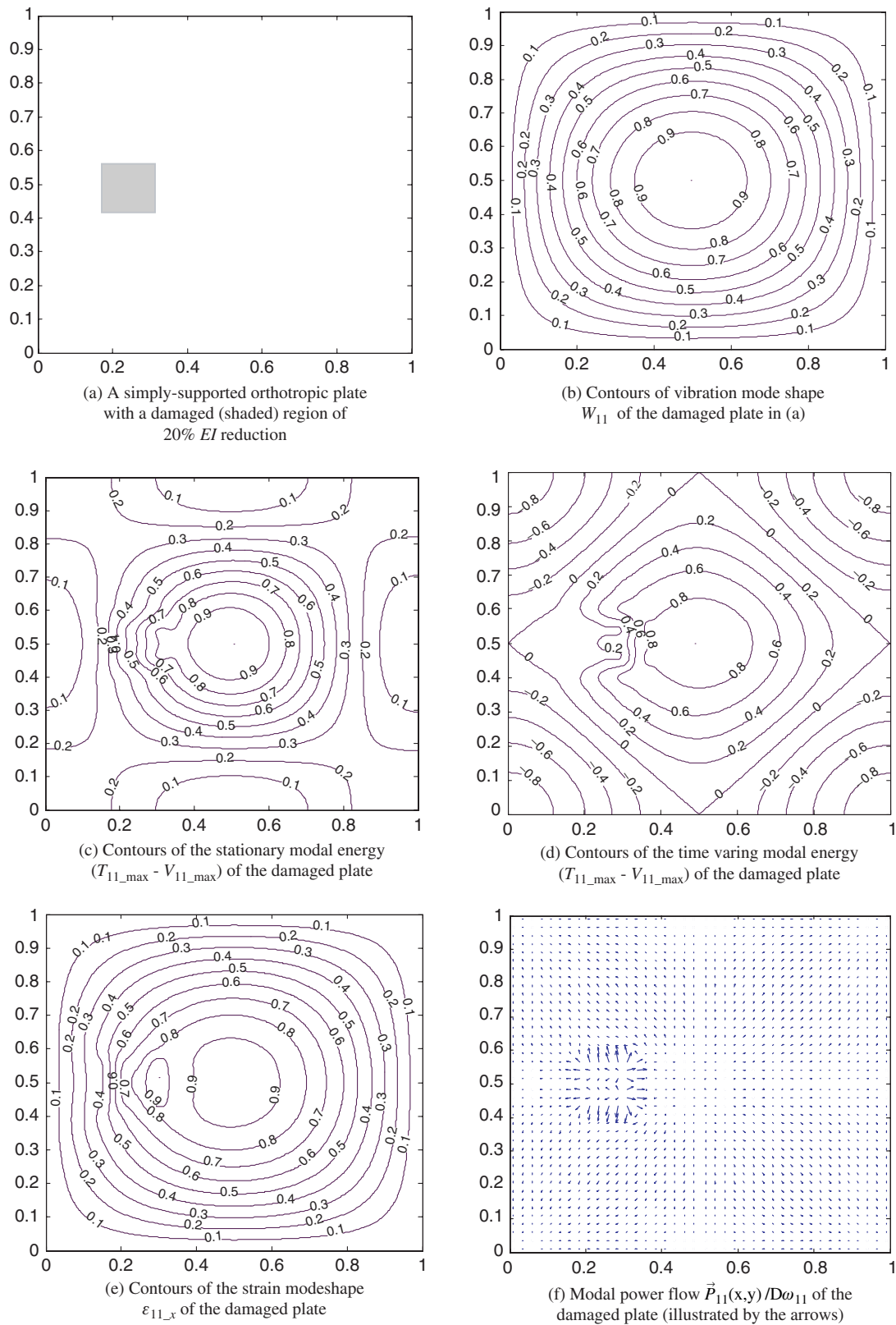


Figure 4. (a) A simply supported orthotropic composite plate with a damaged region of 20% EI reduction; its (b) vibration modeshape; (c) stationary; and (d) time-varying modal energies; (e) strain modeshape; and (f) modal power flow field

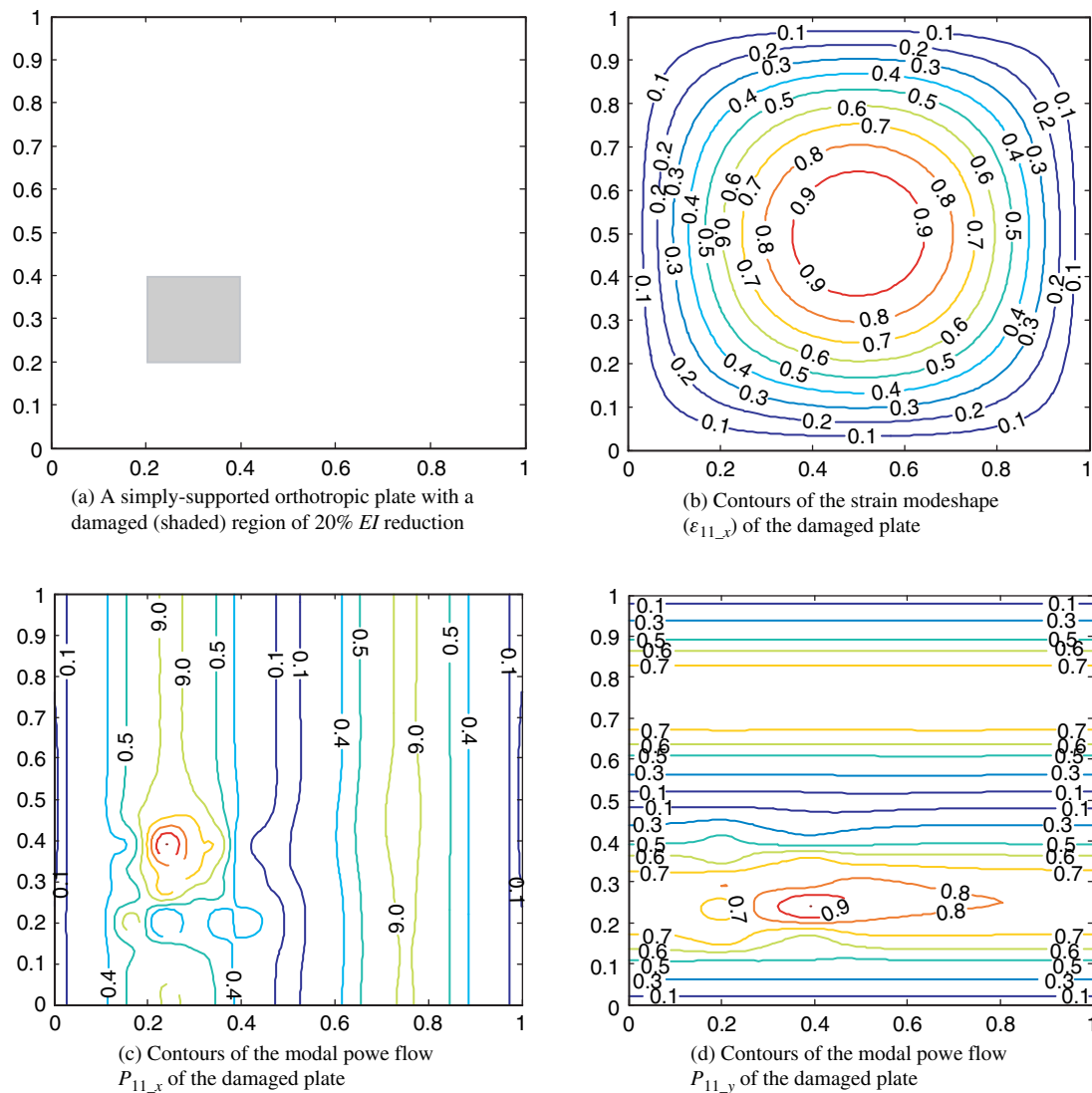


Figure 5. The strain modeshape ϵ_{11_x} , modal power flows P_{11_x} and P_{11_y} of a simply supported orthotropic composite plate with a damaged region of 20% EI reduction

ACKNOWLEDGEMENTS

The authors wish to acknowledge support given to them by the Research Grants Council of The Hong Kong SAR Government through Grant No. PolyU 5340/09E.

REFERENCES

- Alvandi, A. and Cremona, C. (2006). "Assessment of vibration-based damage identification techniques", *Journal of Sound and Vibration*, Vol. 292, No. 1–2, pp. 179–202.
- Chen, H.P. and Bicanic, N. (2000). "Assessment of damage in continuum structures based on incomplete modal information", *Computers and Structures*, Vol. 74, No. 5, pp. 559–570.
- Cornwell, P., Doebling, S.W. and Farrar, C.R. (1999). "Application of the strain energy damage detection method to plate-like structures", *Journal of Sound and Vibration*, Vol. 224, No. 2, pp. 359–374.
- Ewins, D.J. (2000). *Modal Testing: Theory, Practice and Application*, Research Studies Press, Baldock, England.
- Gavric, L. and Pavic, G. (1993). "A finite element method for computation of structural intensity by the normal mode approach", *Journal of Sound and Vibration*, Vol. 164, No. 1, pp. 29–43.
- Khun, M.S., Lee, H.P. and Lim, S.P. (2004). "Structural intensity in plates with multiple discrete and distributed spring-dashpot systems", *Journal of Sound and Vibration*, Vol. 276, No. 3–5, pp. 627–648.
- Lee, H.P., Lim, S.P. and Khun, M.S. (2006). "Diversion of energy flow near crack tips of a vibrating plate using the structural intensity technique", *Journal of Sound and Vibration*, Vol. 296, No. 3, pp. 602–622.
- Li, T.Y., Zhang, W.H. and Liu, T.G. (2001). "Vibrational power flow analysis of damaged beam structures", *Journal of Sound and Vibration*, Vol. 242, pp. 59–68.
- Li, Y.Y., Cheng, L., Yam, L.H. and Wong, W.O. (2002). "Identification of damage locations for plate-like structures using

- damage sensitive indices: strain modal approach”, *Computers & Structures*, Vol. 80, No. 25, pp. 1881–1894.
- Mandal, N.K. and Biswas, S. (2005). “Vibration power flow: a critical review”, *The Shock and Vibration Digest*, Vol. 37, No. 1, pp. 3–11.
- Marks, R.J., II. (1991). *Introduction to Shannon Sampling and Interpolation Theory*, Spinger-Verlag, New York, USA.
- Shi, Z.Y., Law, S.S. and Zhang, L.M. (1998). “Structural damage localization from modal strain energy change”, *Journal of Sound and Vibration*, Vol. 218, No. 5, pp. 825–844.
- Whalen, M.T. (2008). “The behavior of higher order mode shape derivatives in damaged, beam-like structures”, *Journal of Sound and Vibration*, Vol. 309, No. 3–5, pp. 426–464.
- Wong, W.O. (2002). “The effects of distributed mass loading on plate vibration behavior”, *Journal of Sound and Vibration*, Vol. 252, No. 3, pp. 577–583.
- Zou, Y., Tong, L. and Steven, G.P. (2000). “Vibration-based model-dependent damage (delamination) identification and health monitoring for composite structures –a review”, *Journal of Sound and Vibration*, Vol. 230, No. 2, pp. 357–378.

